Alterations in the immuno-skeletal interface drive bone destruction in HIV-1 transgenic rats

Tatyana Vikulina[a,1], Xian Fan[b,c,1], Masayoshi Yamaguchi[a], Susanne Roser-Page[c], Majd Zayzafoon[d], David M. Guidot[b,c], Ighovwerha Ofotokun[e], and M. Neale Weitzmann[a,c,f,2]

Divisions of [a]Endocrinology and Metabolism and Lipids and [b]Pulmonary, Allergy and Critical Care Medicine, Emory University School of Medicine, Atlanta, GA 30322; [c]Atlanta Veterans Affairs Medical Center, Decatur, GA 30033; [d]Department of Pathology, University of Alabama at Birmingham, Birmingham, AL 35294; [e]Division of Infectious Diseases, Department of Medicine, Emory University School of Medicine, Atlanta, GA 30322; and [f]Winship Cancer Institute, Emory University School of Medicine, Atlanta, GA 30322

Edited* by Max D. Cooper, Emory University, Atlanta, GA, and approved June 24, 2010 (received for review March 10, 2010)

Osteoporosis and bone fractures are increasingly recognized complications of HIV-1 infection. Although antiretroviral therapy itself has complex effects on bone turnover, it is now evident that the majority of HIV-infected individuals already exhibit reduced bone mineral density before therapy. The mechanisms responsible are likely multifactorial and have been difficult to delineate in humans. The HIV-1 transgenic rat recapitulates many key features of human AIDS. We now demonstrate that, like their human counterparts, HIV-1 transgenic rats undergo severe osteoclastic bone resorption, a consequence of an imbalance in the ratio of receptor activator of NF-κB ligand, the key osteoclastogenic cytokine, to that of its physiological decoy receptor osteoprotegerin. This imbalance stemmed from a switch in production of osteoprotegerin to that of receptor activator of NF-κB ligand by B cells, and was further compounded by a significantly elevated number of osteoclast precursors. With the advancing age of individuals living with HIV/AIDS, low bone mineral density associated with HIV infection is likely to collide with the pathophysiology of skeletal aging, leading to increased fracture risk. Understanding the mechanisms driving bone loss in HIV-infected individuals will be critical to developing effective therapeutic strategies.

AIDS | osteoprotegerin | osteoporosis | receptor activator of NF-κB ligand | osteoclast

Immune cells are both key regulators of basal bone homeostasis and protagonists of inflammatory bone destruction (1–3). Two archetypal manifestations of aging are loss of immunocompetence and degradation of the skeleton. Interestingly, these pathologic processes are also being recognized as features of HIV infection, and in many respects AIDS recapitulates conditions of accelerated aging (4). Such metabolic alterations may also exacerbate the pathophysiology of natural aging in the AIDS population, leading to amplified or synergistic effects (5). This is of great concern as it is projected that, by the year 2015, more than 50% of the HIV-infected population in the United States will be over the age of 50 y (4). Although highly active antiretroviral therapy (HAART) has been hugely successful in managing HIV/AIDS and increasing mean survival time, osteoporosis (6) and bone fractures (7–9) are now becoming increasingly common. Any fracture can be a significant cause of morbidity (10), and hip fractures almost always require surgery and, in the aged population, are associated with a rate of mortality as high as 30% within the first year (11).

The skeleton is a dynamic organ that is continually renewed by the process of homeostatic bone remodeling. Osteoclasts (OCs), the cells responsible for bone destruction (resorption), form from precursors that circulate within the monocytic population, and are recognized by their expression of receptor activator of NF-κB (RANK). OC precursors differentiate into OCs under the influence of the key osteoclastogenic cytokine RANK ligand (RANKL), and moderated by RANKL's physiological decoy receptor osteoprotegerin (OPG) (12). In humans and animals, any increase in the ratio of RANKL to OPG accelerates the rate of osteoclastic bone resorption. Although, many cell types are capable of making RANKL and OPG, B cells are recognized as a significant source of RANKL when activated in vitro (13), in postmenopausal humans in vivo (3), and in inflammatory conditions such as periodontitis (14). By contrast, both human (15) and mouse B cells (1) are recognized producers of OPG, which is regulated, in part, by T cells through CD40/CD40 ligand (CD40L) costimulation (1, 15). Consequently, B cells and T cells are critical stabilizers of basal peak bone mineral density (BMD) in mice in vivo (1). Furthermore, the entire B-cell lineage including early B cell precursors, immature B cells, mature B cells, and terminally differentiated plasma cells, account for as many as 64% of total bone marrow (BM) OPG concentrations, with mature B cells alone contributing 45% of total BM OPG. Consequently, animal models of B-cell deficiency, T-cell deficiency, and CD40 and CD40L deficiency all undergo significant skeletal deterioration as a result of decreased total OPG concentrations, as a direct consequence of diminished B-cell OPG production (1).

In HIV-1 infection, extensive damage to the immune system occurs, affecting both the cellular and humoral immune responses and leading to severe B-cell exhaustion (16).

Although osteoporosis has long been recognized in patients with HIV/AIDS, the limited capacity to perform mechanistic studies in humans, coupled with myriad copresenting risk factors for osteoporosis, have made it difficult to assess the root causes of altered bone turnover (17). In this study we investigated the impact of HIV-1/AIDS on the skeleton, using HIV-1 transgenic (Tg) rats, an animal model of HIV-1/AIDS involving the global transgenic expression of a HIV-1 gag/pol deleted provirus (18). This model recapitulates many of the immunological and other metabolic complications associated with HIV-1/AIDS in humans, including wasting, skin lesions, cataracts, and pulmonary, immunological, neurological, cardiac, and renal pathologic processes (18–20). We now add osteoporosis to this list of complications, and validate the HIV-1 Tg rat for the study of the mechanisms underlying bone loss in HIV-1/AIDS. Our data highlight perturbations in B cell and monocyte populations as key protagonists driving HIV-induced osteoclastic bone loss in this model.

Results

BMD and Bone Structure Are Severely Altered in HIV Tg Rats. To determine whether HIV Tg rats recapitulate an osteoporotic phenotype as commonly observed in treatment-naive human HIV/AIDS patients, we performed ex vivo dual-energy X-ray absorp-

Author contributions: I.O. and M.N.W. designed research; T.V., X.F., M.Y., S.R.-P., and M.Z. performed research; D.M.G. contributed new reagents/analytic tools; M.N.W. analyzed data; and M.N.W. wrote the paper.

The authors declare no conflict of interest.

*This Direct Submission article had a prearranged editor.

[1]T.V. and X.F. contributed equally to this study.

[2]To whom correspondence should be addressed. E-mail: mweitzm@emory.edu.

This article contains supporting information online at www.pnas.org/lookup/suppl/doi:10.1073/pnas.1003020107/-/DCSupplemental.

tiometry (DXA) on male age-matched (14 mo old) WT and HIV-1 Tg rat femurs (Fig. 1*A*), tibias (Fig. 1*B*), and lumbar spines (Fig. 1*C*). Our data reveal significant reductions in BMD at all sites examined in HIV-1 Tg rats.

To independently assess trabecular and cortical bone structure we analyzed femora from WT and HIV-1 Tg rats by microcomputed tomography (μCT) scan. HIV-1 Tg rats displayed (Table 1) diminished trabecular total volume (TV), indicative of diminished bone size, trabecular bone volume (BV), indicative of diminished bone mass, and decreased BV/TV ratio, suggesting an overall decrease in bone content after normalization for changes in bone size. These decrements in BV were reflected by significant declines in structural indices, including trabecular number and trabecular connectivity density, leading to a corresponding increase in trabecular space. Trabecular thickness was marginally diminished and fell slightly short of statistical significance. Volumetric density measurements confirmed the areal BMD quantification by DXA showing significantly diminished trabecular BMD in the HIV Tg rat. Cortical bone volume showed a significant decrease whereas cortical thickness was not significantly changed.

Scans from representative femurs from each group (WT and HIV-1 Tg) were reconstructed to generate high-resolution longitudinal (Fig. 1*D*) and cross-sectional (Fig. 1*E*) trabecular 3D images, and cortical 3D cross sections (Fig. 1*F*). Trabecular images revealed severely degraded trabecular bone structure and diminished cross-sectional area in the HIV-1 Tg rat femur, whereas cortical images show reduced cortical volume. Overall these data demonstrate a significant decrement in BMD and bone volume in HIV-1 Tg rats.

Table 1. Structural analysis of femurs from HIV-1 Tg and WT rats by μCT

Index	WT rats	HIV-1 rats	Change, %	*P* value*
Trabecular				
TV, mm^3	14.8 ± 1.1	11.5 ± 1.1	−22.4	0.0000001
BV, mm^3	4.9 ± 0.8	2.5 ± 0.5	−47.9	0.0000005
BV/TV, %	33.2 ± 4.0	22.4 ± 4.3	−32.5	0.0000859
Tb. Th, μm	72.1 ± 6.2	65.9 ± 5.3	−8.5	0.0562849
Tb. N/mm	6.6 ± 0.7	4.7 ± 1.0	−29.1	0.0002578
Conn. D., per mm^3	322.2 ± 38.3	264.0 ± 121.7	−18.1	0.0116980
Tb. Sp, μm	199.9 ± 19.8	273.6 ± 53.3	+36.9	0.0015729
TV. D, mg HA/cm^3	405.3 ± 43.5	292.9 ± 54.1	−27.7	0.0003269
Cortical				
Co. Vol, mm^3	8.1 ± 0.3	6.7 ± 1.0	−18.7	0.03296
Co. Th, μm	592.0 ± 81.4	565.2 ± 47.8	−12.5	0.55463

Trabecular indices, including TV, BV, trabecular thickness (Tb. Th.), trabecular space (Tb. Sp.), trabecular number (Tb. No.), trabecular connectivity density (Conn. D.), and cortical indices cortical thickness (Co. Th.) and cortical bone volume (Co. Vol.), were computed from μCT scans. The data are presented as the mean ± SD of 8 WT and 11 HIV-1 rats per group, age 8–9 mo. *Student's *t* test.

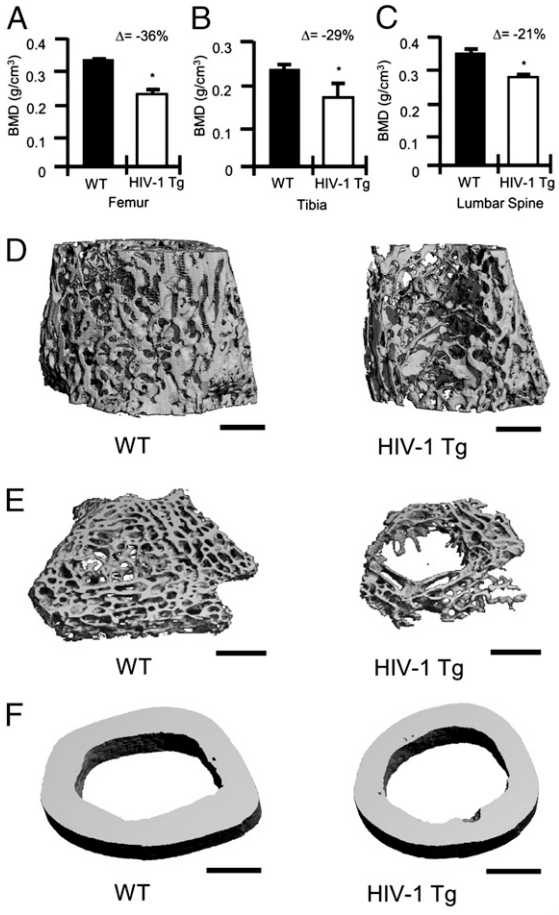

Fig. 1. BMD and bone structure in HIV-1 Tg rats. BMD in (*A*) femurs, (*B*) tibias, and (*C*) lumbar spines were analyzed by DXA ex vivo. The percentage change (Δ) between WT and HIV-1 Tg is indicated for each site. (n = 4 femurs or tibias per group and n = 6 spines per group; average ± SD, *$P \leq 0.05$ by Mann-Whitney test). (*D*) Representative longitudinal trabecular (12 μm), (*E*) cross-sectional (6 μm) trabecular, and (*F*) cortical (12 μm) 3D reconstructions of femurs from WT and HIV-1 Tg rats were generated by μCT. (Scale bar, 1 mm.)

HIV-1 Tg Rats Have Reduced Bone Mass as a Consequence of Increased Osteoclastic Bone Resorption. Our combined structural analyses show a significant decline in BMD and bone architecture in HIV-1 Tg rats relative to their WT littermates, suggesting a diminished bone formation, elevated bone resorption, or both. To assess these possibilities, we quantified in vivo global biochemical markers of bone turnover in rat serum including C-terminal telopeptide of collagen (CTx), and serum osteocalcin, sensitive and specific markers of in vivo bone resorption and formation, respectively. The data demonstrate a significant increase in indices of bone resorption in HIV-1 Tg rats (Fig. 2*A*), whereas no significant change in the marker of bone formation was observed (Fig. 2*B*).

An increase in the number of OCs in HIV-1 Tg rats was confirmed by histologic examination of decalcified tibial sections (Fig. 2 *C*–*F*), and the number of OCs normalized for bone surface area (Fig. 2*G*) and OC surface normalized for bone surface (Fig. 2*H*) was quantitated by histomorphometry using digital imaging and quantitation of cells stained positive (red) for tartrate resistant acid phosphatase (TRAP), a specific marker of the OC phenotype. H&E-stained sections confirm diminished trabecular structure in HIV-1 Tg tibias histologically (Fig. 2 *I* and *J*).

BM from HIV-1 Tg Rats Generates Enhanced Numbers of OCs ex Vitro. In vitro osteoclastogenesis assays were performed using whole BM from HIV-1 Tg and WT rats. BM was cultured ex vivo in the absence (control) and presence of subsaturating (15 ng/mL) or saturating (50 ng/mL) concentrations of RANKL. Cultures were fixed and TRAP-stained to visualize OCs after 7 d. OCs were quantified (Fig. 3*A*) and representative fields photographed (Fig. 3*B*). The data revealed an elevated rate of basal and subsaturating RANKL-induced osteoclastogenesis in HIV-1 Tg BM relative to WT controls, indicative of an enhanced osteoclastogenic environment. Furthermore, addition of saturating concentrations of RANKL continued to evoke significantly increased OC formation in HIV-1 Tg cultures, suggesting the presence of an amplificatory mechanism or an enhanced number of OC precursors.

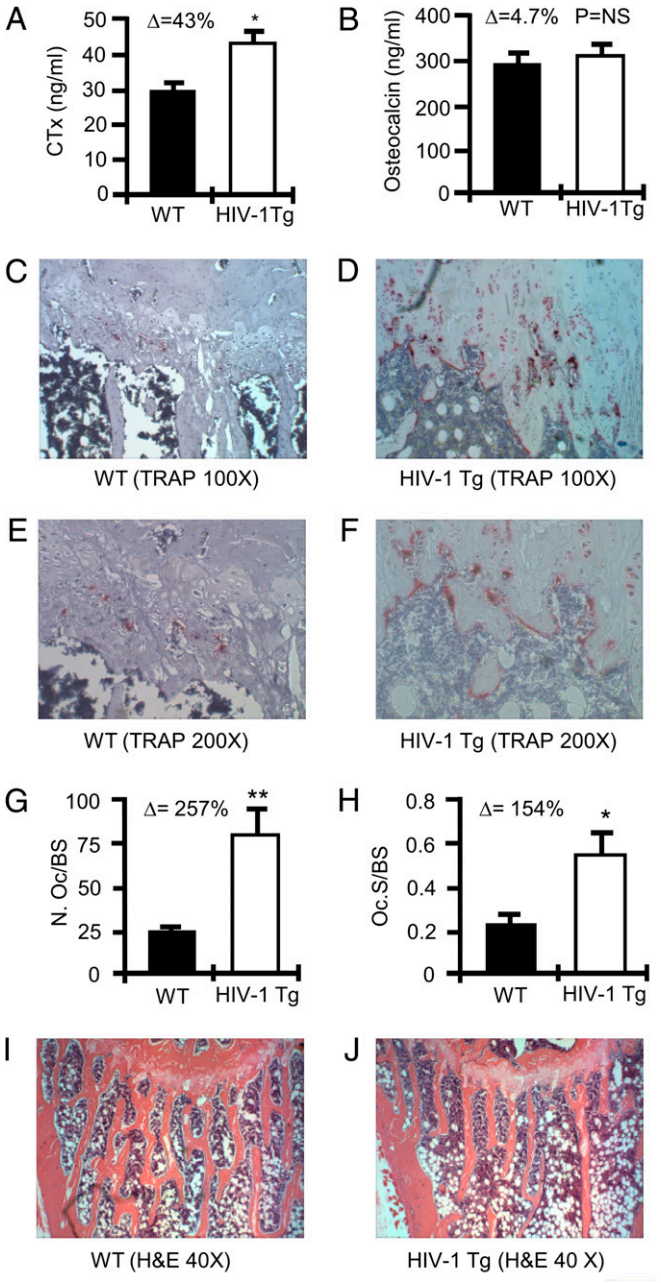

Fig. 2. OCs and bone resorption in HIV-1 Tg rats. (*A*) C-terminal telopeptide (CTx) and (*B*) osteocalcin were quantified in the serum of WT and HIV Tg rats. (*$P \leq 0.002$ by *t* test; $n = 4$ rats per group). Histology and histomorphometry for OCs were performed in tibias. Representative TRAP-stained tibia sections are shown for WT rats (*C* and *E*) and HIV-1 Tg rats (*D* and *F*) at magnifications of 100× (*C* and *D*) and 200× (*E* and *F*). (*G*) The number of OCs per bone surface area (N.Oc/BS); and (*H*) OC surface per bone surface area (Oc.S/BS) was calculated as mean ± SD of five WT and six HIV-1 Tg rats (*$P = 0.03$, **$P = 0.0095$ by *t* test). H&E-stained tibias for WT (*I*) and HIV-1 Tg (*J*) rats at 40× magnification. Mineralized bone stains orange/pink.

TNF-α is a cytokine known to amplify the osteoclastogenic activity of RANKL (21–23). Serum levels of TNF-α have been reported to be elevated in patients with HIV, and are suggested to play a critical role in the clinical progression of HIV infection (30). To determine whether elevated levels of TNF-α play a role in the enhanced osteoclastogenic activity in HIV-1 Tg rats, we cultured OCs ex vivo in the presence of a subsaturating dose of RANKL (15 ng/mL) in the presence or absence of a saturating dose of neutralizing TNF-α antibody (20 μg/mL). TNF-α neutralization failed to alter the enhanced osteoclastogenic activity of BM from HIV-1 Tg rats (Fig. 3*C*). By contrast recombinant TNF-α significantly amplified RANKL-induced osteoclastogenesis in both control and HIV-1 Tg rat BM.

As TNF-α has been reported to be elevated in serum from human patients with HIV, we further performed an ELISA for TNF-α on WT and HIV-1 Tg rat serum. Unlike in human HIV, serum levels of TNF-α were not significantly elevated in HIV-1 Tg (8.0 ± 0.3 pg/mL) rat serum relative to WT (mean ± SD, 8.2 ± 0.6 pg/mL; $n = 10$ rats per group measured independently and averaged).

To determine whether the enhanced osteoclastogenic activity of HIV-1 Tg BM was associated with an enhanced number of OC precursors, we quantified the number of OC precursors (defined as $CD11b^+RANK^+$ cells) in the BM using flow cytometry. A significant increase in the number of OC precursors was observed in HIV-1 Tg BM compared with WT controls (Fig. 3*D*). Interestingly, FACS analysis also revealed a significant reduction (percentage change, −45.7%) in macrophages (Fig. 3*E*), suggesting a block in monocyte differentiation into macrophages leading to a pooling of monocytes and OC precursors.

As HIV-1 infection is reported to promote macrophage colony-stimulating factor (M-CSF) production by macrophages (24), elevated M-CSF could account for the enhanced levels of OC precursors observed by FACS in HIV-1 Tg rats. We thus quantified M-CSF expression by real-time RT-PCR in whole BM from WT and HIV-1 Tg rats. M-CSF expression was found to be increased by approximately 2.5-fold in HIV-1 Tg rats (Fig. 3*F*).

HIV-1 Transgenic Rats Display Diminished Total OPG and Elevated Total RANKL Production. OC formation and bone resorption are a function of the ratio of RANKL to that of OPG. To assess osteoclastogenic cytokine production, we quantified total splenic (Fig. 4*A*) and BM (Fig. 4*C*) RANKL mRNA expression and total splenic (Fig. 4*B*) and BM (Fig. 4*D*) OPG mRNA expression in WT and HIV-1 Tg rats by using real-time RT-PCR. A significant increase in total RANKL expression was observed in HIV-1 Tg rats, concomitant with a significant decline in total OPG expression in both BM and spleen.

Transition from OPG to RANKL Production by B Cells in HIV-1 Tg Rats. Because B cells are a major OPG-producing population under basal conditions, but secrete RANKL when activated or under inflammatory conditions, we immunomagnetically purified splenic B cells as previously described (1) and quantified RANKL (Fig. 4*E*) and OPG (Fig. 4*F*) mRNA expression by real-time RT-PCR. The data revealed a significant increase in B cell RANKL mRNA expression coupled with a severe decline in B-cell OPG production. Although T cells are also a major component of spleen and a potential source of RANKL, no significant changes in RANKL (Fig. 4*G*) or OPG (Fig. 4*H*) expression was observed in the non-B cell–containing fraction.

Discussion

Our characterization of the skeleton and bone turnover in HIV-1 Tg rats ratifies this model for the study of bone turnover and osteoporosis in HIV-1/AIDS. Our data reveal a significant decrease in BMD and bone volume in HIV-1 Tg rats. Unlike mice and humans, the skeletons of rats continue to grow in size throughout life. Analysis of trabecular and cortical tissue volume with μCT reveals that the bones of HIV-1 Tg rats are significantly smaller than their WT counterparts. This is consistent with development of a wasting syndrome and diminished body mass in HIV-1 Tg rats. Indeed, muscle atrophy is another metabolic complication of HIV/AIDS that is replicated in the HIV-1 Tg rat. As BMI is an established predictor of BMD, weight loss may thus contribute to bone loss in our model. In fact, at 11 mo of age, our HIV-1 Tg rats weighed an average of 21% less than WT controls, although no

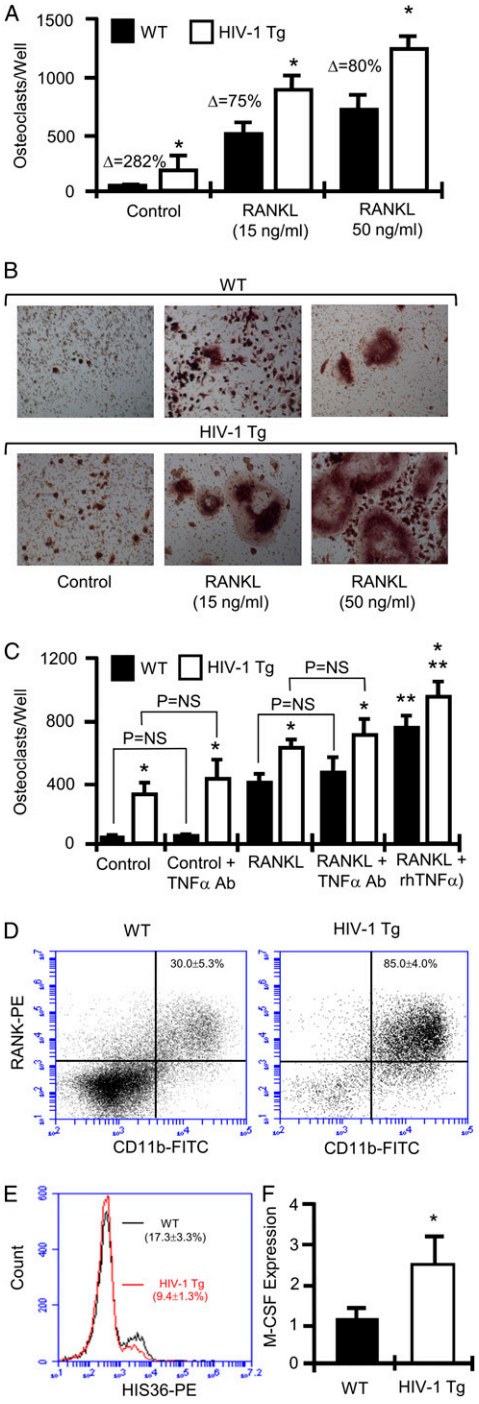

Fig. 3. In vitro OC formation and quantification of OC precursors. (*A*) OCs were cultured from BM isolated from WT and HIV-1 Tg rats in the absence of RANKL (control), subsaturating concentrations of RANKL (15 ng/mL), and saturating concentrations of RANKL (50 ng/mL). TRAP positive multinucleated cells were scored as OCs. Mean ± SD of three independent experiments with six wells per data set each. (n = 2 rats/group pooled for each experiment; *$P < 0.01$ on one-way ANOVA with Tukey-Kramer post-test; Δ, percentage change from WT.) (*B*) Photomicrographs of representative OC cultures. (*C*) OCs were cultured from BM isolated from WT and HIV-1 Tg rats in the presence or absence of RANKL (15 ng/mL) and neutralizing antibody to TNF-α (TNF-α Ab; 20 μg/mL) or rmTNF-α (2.5 ng/mL). TRAP-positive multinucleated cells (≥3 nuclei) were scored as OCs. Mean ± SD of two independent experiments of six wells per data set each. (n = 1 rat per group for each experiment; *$P < 0.001$ vs. WT, **$P < 0.001$ vs. RANKL only, P = not significant, one-way ANOVA with Tukey-Kramer post test.) (*D*) FACS analysis of OC precursors ($CD11b^+RANK^+$ cells) and (*E*) $HIS36^+$ macrophages. (*F*) Real-time RT-PCR for whole BM M-CSF expression. (Mean ± SD of five rats per group assayed independently; *$P = 0.032$, Mann-Whitney test.)

obvious differences in food and water consumption were noted. Mechanical loading associated with body mass has long been considered to promote bone formation, although more recently hormonal cues such as leptin-mediated suppression of osteoblastogenesis is further reported to link body mass index to BMD through regulation of bone formation, via the sympathetic nervous system (25). In the HIV-1 Tg rat, despite evidence of mild muscle atrophy, biochemical indices of bone turnover suggested that bone formation was not impacted and that diminished bone size and BMD and volume were likely a direct consequence of an elevated rate of osteoclastic bone resorption leading to a net bone loss, and blunting of skeletal growth. However, one may argue that the absence of a normal compensatory increase in bone formation in response to elevated resorption, a consequence of coupling, may be evidence of a coexisting suppressive action on bone formation. Whether loss of coupling is a consequence of a direct imbalance in mechanical loading through reduced BMI, aberrant neurological and/or enhanced leptin production, or a combination of these and other mechanisms remain to be determined.

Our data further suggest that enhanced osteoclastic bone loss may stem from an immunological disruption in basal B cell function leading to a "switch" from expression of the osteoclastogenesis inhibitory factor OPG to expression of the osteoclastogenesis stimulatory factor RANKL. Indeed, dramatic changes are known to occur within the B cell compartment of HIV-1–infected humans, including declines in resting memory B cell populations and increases in naive and immature/transitional B cells (26, 27). The relevant B cell populations responsible for elevated RANKL and/or diminished OPG production remain to be determined; however, it is likely that activated mature B cells, a population whose numbers are increased in association with HIV infection (26), are responsible for RANKL production, whereas resting memory B cells, a population that decreases in HIV infection (26), may account for diminished OPG production.

We (1) and others (15) have reported that CD40/CD40L costimulation between B cells and T cells up-regulates OPG production. Consequently, changes in OPG production in HIV/AIDS may be a consequence, in part, of defective T-cell costimulation. In X-linked hyper-IgM syndrome, an immunodeficiency with significant similarities to HIV-1 infection, including osteopenia, $CD27^+B220^-$ memory B cells are preferentially depleted as a consequence of defective CD40L expression by activated T cells, preventing normal T-cell to B-cell interactions (27). Interestingly, viral gp120 association with CD4 on T cells also suppresses CD40L expression during T cell activation in HIV-1 infection (27). These data suggest that disruption of B-cell function and/or depletion of $CD27^+B220^-$ memory B cells may be associated with the etiology of osteoporosis in HIV/AIDS.

Ultimately, these questions cannot be addressed in the rat model because of the lack of specific markers necessary to identify the different cell populations in rodents. Future studies will need to be undertaken using human tissues to ratify the animal data and to more comprehensively investigate the nature of the specific B-cell populations and subtypes involved.

In addition to anomalous B-cell function, our data further suggest that osteoclastogenesis promoted by the elevated RANKL/OPG ratio is further intensified by a significant increase in the concentration of available OC precursors in the BM of HIV-1 Tg rats. Our data suggest that a block in the transition of monocytes to macrophages may lead to a pooling of monocytes and OC precursors. These data are consistent with studies of HIV infection in humans and SIV infection in rhesus macaques in which a high turnover state causes an elevation in the concentration of mono-

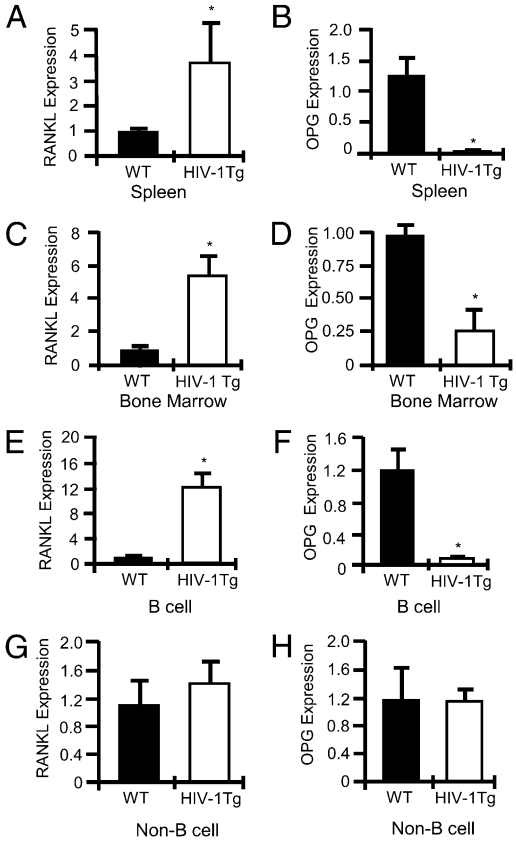

Fig. 4. Total and B cell RANKL and OPG expression in HIV-1 Tg rat spleen and BM. Real-time RT-PCR for RANKL in whole spleen (*A*) and BM (*C*), and for OPG in whole spleen (*B*) and BM (*D*). RANKL (*E*) and OPG (*F*) expression in purified splenic B cells. RANKL (*G*) and OPG (*H*) expression by B cell–depleted splenocytes. (*$P < 0.002$ by *t* test, $n = 4$ rats per group.)

cytes generated in the BM to compensate for a high rate of macrophage destruction in the periphery (28, 29). We furthermore detected a 2.5-fold elevation in expression of M-CSF, a cytokine that supports the proliferation of OC precursors (12), and that likely contributes to the elevated concentrations of OC precursor in our model. These data are further consistent with human studies demonstrating that HIV-1 infection promotes M-CSF production by macrophages (24). Despite the absence of viral replication in the rat model, the data appear consistent with reported effects of SIV and HIV-1 and would support an increased number of OC precursors as an exacerbating force in HIV-induced bone loss.

Surprisingly, TNF-α, a potent amplifier of RANKL-induced osteoclastogenesis (21–23), was not seen to be up-regulated in the serum of HIV-1 Tg rats, and neutralization of TNF-α failed to suppress the enhanced basal and RANKL-stimulated osteoclastogenesis ex vivo. TNF-α is reported to be up-regulated in the serum of human patients with HIV and may play a critical role in the clinical progression of HIV infection (30). It is possible that the transgenic expression of HIV-1 proteins in this model bypasses or negates the requirement for TNF-α in disease progression. However, elevated TNF-α may additionally amplify osteoclastogenesis in the human system.

As the skeleton is exquisitely sensitive to numerous pathological disruptions in the body, it is likely that additional actions such as hormonal imbalances, inflammatory cytokines, and neurological, cardiac, muscle, and renal pathologic processes may all feedback on the skeleton, exacerbating bone loss in HIV-1 Tg rats and/or in humans.

Although loss of BMD is observed in two thirds of HIV-1–seropositive individuals naive to antiretroviral therapy (31), initiation of HAART itself leads to additional bone loss (9, 32). The etiology and causes of HAART-associated bone loss are poorly understood and await further elucidation. However, a limitation of the HIV-1 Tg rat model is that HIV-1 proteins are synthesized transgenically, and expression is constitutive and not impacted by antiretroviral agents. This model is thus not suitable for direct examination of HAART on bone turnover, and consequently our study specifically deal with the disruption in bone turnover associated with HIV-1 infection/AIDS, and does not address the additional impact of HAART on bone turnover.

In summary, as life expectancy for HIV-infected individuals continues to increase as a result of successful therapy with antiretroviral agents, damage sustained by the skeleton from the chronic effect of HIV infection is likely to be exacerbated by age-associated decline in BMD. Thus, the synergistic impact of HIV/AIDS and aging on an already impoverished skeleton could lead to a rapid and massive bone loss, leading to osteoporotic bone fractures among aging patients with HIV/AIDS. Our studies open a window to help explain the underlying causes of bone loss in HIV/AIDS, and will hopefully lead to novel strategies to forestall an epidemic of future bone disease in this population.

Methods

For an expanded description of materials and methods in the present study, see *SI Methods*.

HIV-1 Transgenic Rats. Male hemizygous NL4-3Δgag/pol Fischer 344 rats (HIV-1 Tg; Harlan) have been previously described in detail (18, 20).

Real Time RT-PCR. Real Time RT-PCR was performed using rat specific primer sets for OPG, RANKL, M-CSF, β-actin, and phosphoglycerate kinase (PGK) on an ABI Prism 7000 instrument (Applied Biosystems) as described (1).

In Vitro Osteoclastogenesis Assays. Whole BM was treated with rmM-CSF (30 μg/mL), and rhRANKL (RANKL) at subsaturating doses (15 ng/mL) or saturating doses (50 ng/mL). Some cultures received rmTNF-α (2.5 ng/mL) or neutralizing TNF-α antibody (20 μg/mL). After 7 to 10 d, TRAP+ multinucleated cells (≥3 nuclei) were quantified under light microscopy.

Bone Mineral Density. Ex vivo BMD measurements were performed in rats at 14 mo of age by DXA using a PIXImus2 bone densitometer (GE Medical Systems).

μCT. Rats 8 to 9 mo of age underwent μCT using a μCT 40 scanner (Scanco Medical). For trabecular bone, 70 tomographic slices were taken (total area of 840 μm) at the right distal femoral metaphysis at a resolution of 12 μm (70 KV and 114 μA). Cortical bone was quantified at the mid-diathesis from 100 slices at a resolution of 12 μm. Representative samples were reconstructed in 3D at 12 μm or 6 μm as indicated in the legend to Fig. 1.

Biochemical Indices of Bone Resorption. CTx and serum osteocalcin were measured in rats 8 to 9 mo of age using RATlaps and Rat-MID ELISAs, respectively (Immunodiagnostic Systems).

Cell Purification for RANKL and OPG Quantification. Splenic B cells were immunomagnetically purified using antirat IgM-conjugated microbeads according to the manufacturer's protocol (Miltenyi Biotech).

Statistical Analysis. Simple comparisons were made using unpaired two-tailed Student *t* test for parametric data or Mann-Whitney test for nonparametric data. Multiple comparisons were made using one-way ANOVA with Tukey-Kramer post-test. $P \leq 0.05$ was considered statistically significant. All data are presented as mean ± SD.

ACKNOWLEDGMENTS. We thank Xiaoying Yang for technical assistance with μCT. We gratefully acknowledge the histological services of the University of Alabama at Birmingham, Center for Metabolic Bone Disease–Histomorphometry and Molecular Analysis Core Laboratory, supported by National Institutes of Health Grant P30-AR46031. This study was supported in part by National Institute of Arthritis and Musculoskeletal and Skin Dis-

eases Grants AR059364 (to M.N.W. and I.O.) and AR053607 (to M.N.W.). M.N.W. was also supported in part by National Institute of Arthritis and Musculoskeletal and Skin Diseases Grant AR056090 and Biomedical Laboratory Research and Development Service of the Veterans Affairs Office of Research and Development Grant 5I01BX000105. I.O. was also supported in part by National Institute of Allergy and Infectious Diseases Grant K23 A1073119 and National Institute of Arthritis and Musculoskeletal and Skin Diseases Grant MZ AR053898.

1. Li Y, et al. (2007) B cells and T cells are critical for the preservation of bone homeostasis and attainment of peak bone mass in vivo. *Blood* 109:3839–3848.
2. Weitzmann MN, Pacifici R (2006) Estrogen deficiency and bone loss: An inflammatory tale. *J Clin Invest* 116:1186–1194.
3. Eghbali-Fatourechi G, et al. (2003) Role of RANK ligand in mediating increased bone resorption in early postmenopausal women. *J Clin Invest* 111:1221–1230.
4. Deeks SG (2009) Immune dysfunction, inflammation, and accelerated aging in patients on antiretroviral therapy. *Top HIV Med* 17:118–123.
5. Nguyen N, Holodniy M (2008) HIV infection in the elderly. *Clin Interv Aging* 3: 453–472.
6. Thomas J, Doherty SM (2003) HIV infection—a risk factor for osteoporosis. *J Acquir Immune Defic Syndr* 33:281–291.
7. Guaraldi G, et al. (2001) Pathological fractures in AIDS patients with osteopenia and osteoporosis induced by antiretroviral therapy. *AIDS* 15:137–138.
8. Triant VA, Brown TT, Lee H, Grinspoon SK (2008) Fracture prevalence among human immunodeficiency virus (HIV)-infected versus non-HIV-infected patients in a large U.S. healthcare system. *J Clin Endocrinol Metab* 93:3499–3504.
9. Yin MT, et al. (2010) Low bone mass and high bone turnover in postmenopausal human immunodeficiency virus-infected women. *J Clin Endocrinol Metab* 95:620–629.
10. Johnell O, Kanis JA (2006) An estimate of the worldwide prevalence and disability associated with osteoporotic fractures. *Osteoporos Int* 17:1726–1733.
11. Lewis JR, Hassan SK, Wenn RT, Moran CG (2006) Mortality and serum urea and electrolytes on admission for hip fracture patients. *Injury* 37:698–704.
12. Teitelbaum SL (2000) Bone resorption by osteoclasts. *Science* 289:1504–1508.
13. Choi Y, et al. (2001) Osteoclastogenesis is enhanced by activated B cells but suppressed by activated CD8(+) T cells. *Eur J Immunol* 31:2179–2188.
14. Kawai T, et al. (2006) B and T lymphocytes are the primary sources of RANKL in the bone resorptive lesion of periodontal disease. *Am J Pathol* 169:987–998.
15. Yun TJ, et al. (1998) OPG/FDCR-1, a TNF receptor family member, is expressed in lymphoid cells and is up-regulated by ligating CD40. *J Immunol* 161:6113–6121.
16. Moir S, Fauci AS (2009) B cells in HIV infection and disease. *Nat Rev Immunol* 9: 235–245.
17. Mondy K, et al. (2003) Longitudinal evolution of bone mineral density and bone markers in human immunodeficiency virus-infected individuals. *Clin Infect Dis* 36: 482–490.
18. Reid W, et al. (2001) An HIV-1 transgenic rat that develops HIV-related pathology and immunologic dysfunction. *Proc Natl Acad Sci USA* 98:9271–9276.
19. Reid W, et al. (2004) HIV-1 transgenic rats develop T cell abnormalities. *Virology* 321: 111–119.
20. Lassiter C, et al. (2009) HIV-1 transgene expression in rats causes oxidant stress and alveolar epithelial barrier dysfunction. *AIDS Res Ther* 6:1.
21. Cenci S, et al. (2000) Estrogen deficiency induces bone loss by enhancing T-cell production of TNF-alpha. *J Clin Invest* 106:1229–1237.
22. Lam J, et al. (2000) TNF-alpha induces osteoclastogenesis by direct stimulation of macrophages exposed to permissive levels of RANK ligand. *J Clin Invest* 106:1481–1488.
23. Zhang YH, Heulsmann A, Tondravi MM, Mukherjee A, Abu-Amer Y (2001) Tumor necrosis factor-alpha (TNF) stimulates RANKL-induced osteoclastogenesis via coupling of TNF type 1 receptor and RANK signaling pathways. *J Biol Chem* 276:563–568.
24. Haine V, Fischer-Smith T, Rappaport J (2006) Macrophage colony-stimulating factor in the pathogenesis of HIV infection: Potential target for therapeutic intervention. *J Neuroimmune Pharmacol* 1:32–40.
25. Takeda S, et al. (2002) Leptin regulates bone formation via the sympathetic nervous system. *Cell* 111:305–317.
26. Moir S, et al. (2008) Evidence for HIV-associated B cell exhaustion in a dysfunctional memory B cell compartment in HIV-infected viremic individuals. *J Exp Med* 205: 1797–1805.
27. Morrow M, Valentin A, Little R, Yarchoan R, Pavlakis GN (2008) A splenic marginal zone-like peripheral blood CD27+B220- B cell population is preferentially depleted in HIV type 1-infected individuals. *AIDS Res Hum Retroviruses* 24:621–633.
28. Kim WK, et al. (2009) Monocyte heterogeneity underlying phenotypic changes in monocytes according to SIV disease stage. *J Leukoc Biol* 87:557–567.
29. Hasegawa A, et al. (2009) The level of monocyte turnover predicts disease progression in the macaque model of AIDS. *Blood* 114:2917–2925.
30. Kim SY, Solomon DH (2010) Tumor necrosis factor blockade and the risk of viral infection. *Nat Rev Rheumatol* 6:165–174.
31. Borderi M (2006) Multifactorial relations between HIV, HAART and bone metabolism. *Infez Med* 14:117–124.
32. Tebas P, et al. (2000) Accelerated bone mineral loss in HIV-infected patients receiving potent antiretroviral therapy. *AIDS* 14:F63–F67.